Adam Causse

Aerodynamic performance of the HondaJet

Faculty of Engineering and Applied Sciences
Computational Aerodynamics

MSc
Academic Year: 2025–2026

Supervisors: Dr. Tom-Robin Teschner
August 2025

Faculty of Engineering and Applied Sciences
Computational Aerodynamics

MSc

Academic Year: 2025–2026

Adam Causse

Aerodynamic performance of the HondaJet

Supervisors: Dr. Tom-Robin Teschner
August 2025

This thesis is submitted in partial fulfilment of the requirements for the degree of MSc.

Academic Integrity Declaration

I declare that:

- the thesis submitted has been written by me alone.
- the thesis submitted has not been previously submitted to this university or any other.
- that all content, including primary and/or secondary data, is true to the best of my knowledge.
- that all quotations and references have been duly acknowledged according to the requirements of academic research.

I understand that to knowingly submit work in violation of the above statement will be considered by examiners as academic misconduct.

Abstract

This study presents a comparative numerical investigation of a reverse-engineered HondaJet configuration simulated with and without engines. Reynolds-Averaged Navier–Stokes simulations were conducted using the k–ω SST turbulence model over a Mach number range from 0.70 to 0.84 and for angles of attack between 0° and 10°. The aerodynamic performance of both configurations was evaluated in terms of lift and drag coefficients, as well as pressure coefficient distributions along the wing. The numerical results highlight the impact of the engine installation on the overall aerodynamic behaviour of the aircraft.

Keywords:
CFD simulation, HondaJet HA-420, aerodynamic performance

Acknowledgements

I express my sincere gratitude to my professor for the knowledge, guidance, and support they have provided throughout this project and during our time in the program.

Dr. Tom-Robin Teschner

Contents

List of Figures

List of Tables

List of Abbreviations

RANS	Reynolds-averaged Navier–Stokes
c	Local chord length
C_p	Pressure coefficient
C_d	Drag coefficient
C_l	Lift coefficient
BoI	Body of Influence
OTWEM	Over-the-Wing Engine Mount
Re	Reynolds number
AoA	Angle of attack
M	Mach number

Chapter 1

Introduction

Over the past two decades, the business aviation sector has undergone a major transformation, driven by a growing demand for more energy-efficient and environmentally friendly aircraft. Light business jets occupy a crucial market segment, offering a flexible alternative to commercial airlines while meeting the increasing mobility needs of executives and corporations. However, this segment faces significant challenges: reducing fuel consumption, lowering pollutant emissions, and improving cruise performance have become decisive criteria for competitiveness and economic viability.

The HondaJet HA-420 represents a significant breakthrough in the design of light business jets. Unlike conventional architectures, this aircraft incorporates several remarkable aerodynamic innovations that position it as a technological leader in its category. Its most distinctive feature is the over-the-wing engine mount (OTWEM) system, a novel approach that departs radically from established design conventions. This configuration is not merely aesthetic; it offers potential aerodynamic benefits by reducing interference effects between the engine nacelles and the fuselage, while optimizing the airflow around the lifting surfaces.

The objective of this study is to assess, through CFD simulations, the aerodynamic performance of the HondaJet HA-420 under nominal cruise conditions, with a particular focus on comparing the configuration with over-the-wing engine mounting to a configuration without engines. This investigation aims to quantify the actual impact of the OTWEM innovation on cruise flight performance phase in which energy efficiency is paramount for both range and operational economics.

Chapter 2

Literature review

The HondaJet HA420 is the result of extensive aerodynamic research and design studies. Fujino[3], Yoshizaki, and Kawamura conducted a detailed investigation into the development of Natural Laminar Flow (NLF) airfoils, focusing on the SHM-1 airfoil profile. Their results demonstrated a drag divergence Mach number exceeding 0.7, highlighting the suitability of this airfoil for high-subsonic cruise conditions. These performance levels are comparable to those obtained by Somers[4], who proposed a thinner NLF slotted airfoil configuration, also achieving a drag divergence Mach number above 0.7, consistent with typical cruise speeds of light business jets.

During the development of the HondaJet, Fujino[1] further conducted a design study comparing the lift coefficient of the wing with and without Over-The-Wing Engine Mount (OTWEM) configuration. The results showed a slight reduction in lift coefficient when the engine was installed above the wing, indicating a moderate aerodynamic penalty associated with engine integration.

In parallel, Blaesser[5], Schetz, and Kapania investigated the optimal engine placement in the context of the emergence of Ultra-High Bypass Ratio (UHBR) engines, which are characterized by significantly larger diameters. Their study demonstrated that the OTWEM configuration yielded the most favorable results in terms of drag, minimizing the aerodynamic impact of engine positioning on the overall aircraft performance.

Chapter 3

Methodology

3.1 Meshing Strategy

The meshing strategy adopted in this study is based on a previous project involving the simulation of a Saab 340[2] aircraft. Several *body-of-influence* (BoI) regions are defined around the aircraft, the engine, and the winglet. The purpose of these regions is to locally refine the mesh in order to better capture the aerodynamic effects of these areas, particularly their contribution to drag.

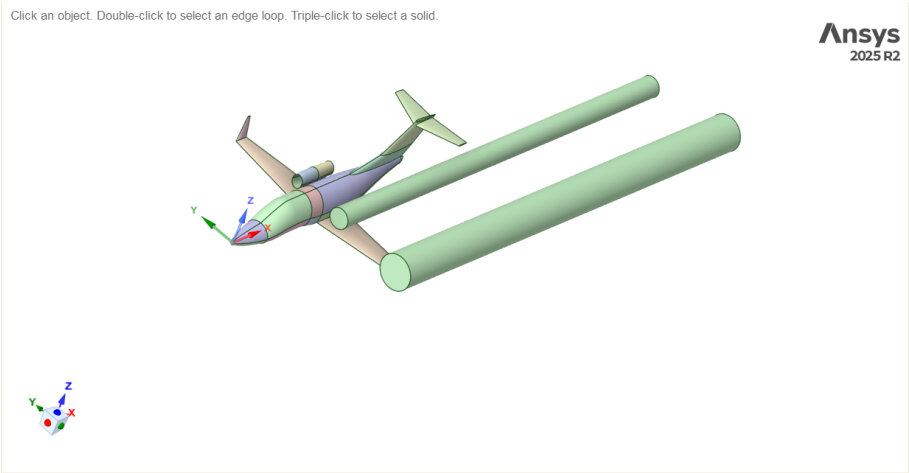

Figure 3.1: Body-of-influence regions used for mesh refinement

The aircraft geometry is divided into four main parts: the fuselage; the wing, horizontal stabiliser, vertical stabiliser, and engine pylon; the engine; and the edges, which correspond to small surfaces located at the wingtips, horizontal stabiliser tips, and engine pylon junctions.

All mesh sizes and meshing strategies are summarised in Table 3.1. These parameters are directly inherited from the Saab 340[2] numerical model in order to ensure consistency with previous validated simulations.

Table 3.1: Mesh settings and size functions[2]

Mesh Part	Size Function	Settings
Inlet, Outlet, Symmetry, Farfield	Face Size	Target mesh size: 10000 mm
BoI – wake	Body-of-Influence	Value: 500 mm
BoI – wingtip	Body-of-Influence	Value: 100 mm
Fuselage	Curvature	Min: 10 mm Max: 100 mm Curvature normal angle: 15°
Engine	Curvature	Min: 10 mm Max: 100 mm Curvature normal angle: 15°
Wing, Horizontal Stabiliser, Vertical Stabiliser, Nacelle Fixation	Curvature	Min: 5 mm Max: 75 mm Curvature normal angle: 15°
Edges	Face Size	Target mesh size: 2 mm

3.2 Simulation Setup

Each simulation is run for 4000 iterations using the k–ω *SST* turbulence model.

3.2.1 Atmospheric Conditions

The simulations are performed under cruise flight conditions at an altitude of 30 000 ft[6]. The atmospheric parameters are defined according to the International Standard Atmosphere (ISA), assuming a reference sea-level temperature of 15°C.

The physical properties used in the simulations and their corresponding values are summarised in Table 3.2.

Table 3.2: Atmospheric conditions at 30 000 ft (ISA)

Property	Value
Altitude [ft]	30 000
Temperature [K]	228.71
Pressure [Pa]	30 070
Density [kg m^{-3}]	4.581×10^{-1}
Speed of sound [m s^{-1}]	303.0
Dynamic viscosity [Pa s]	1.487×10^{-5}

Chapter 4

Results and Discussion

4.1 Comparison with Experimental Data

4.1.1 Drag Coefficient

The first comparison is performed by plotting the drag coefficient C_d as a function of the Mach number.

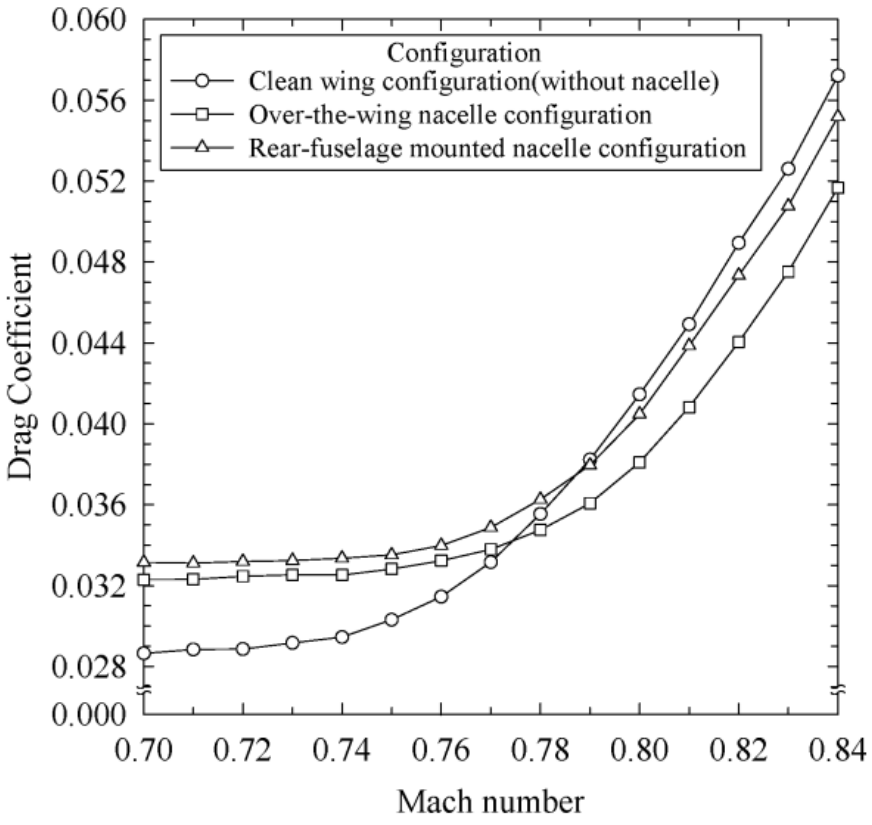

Figure 4.1: Experimental drag coefficient as a function of Mach number[1]

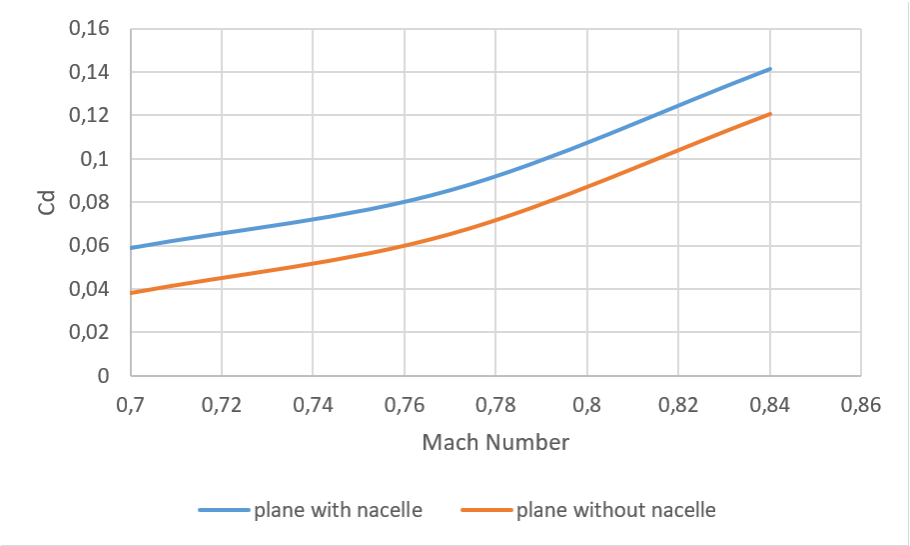

Figure 4.2: Numerical drag coefficient as a function of Mach number (k–ω SST model)

The drag coefficient obtained from the numerical simulation is approximately twice as large as the experimentally measured value. Moreover, the intersection of the drag curves observed in the experimental data is not reproduced by the present simulation. This discrepancy suggests limitations in the numerical setup, which may be related to the turbulence modelling, mesh resolution, or boundary condition assumptions.

4.1.2 Lift Coefficient

The experimental lift measurements were conducted at a significantly lower Mach number than the numerical simulations. Indeed, the experimental data were obtained at $M = 0.186$, whereas the simulations were performed at $M = 0.7$. However, the Reynolds numbers are very similar, with values of 10.3×10^6 for the experimental case and 10.2×10^6 for the numerical simulation. Consequently, a comparison between the two datasets remains relevant.

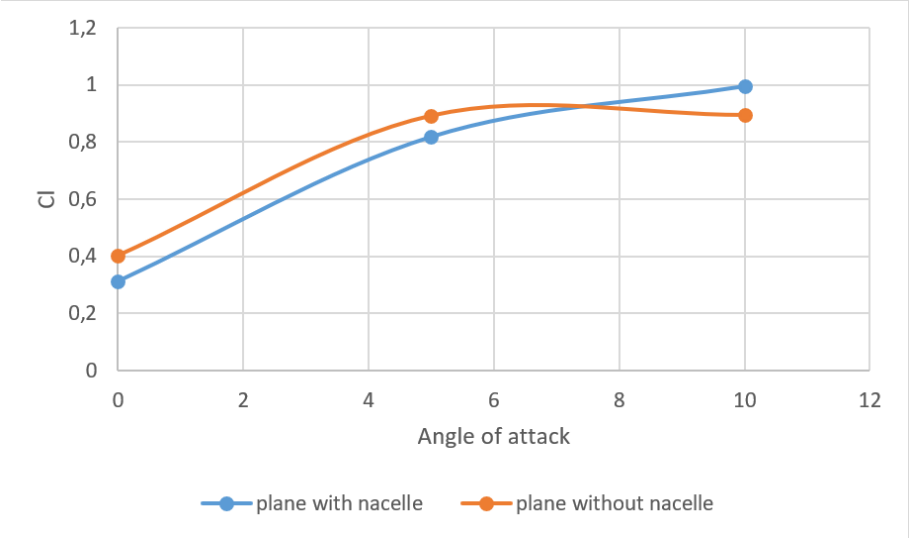

Figure 4.3: Numerical lift coefficient as a function of angle of attack

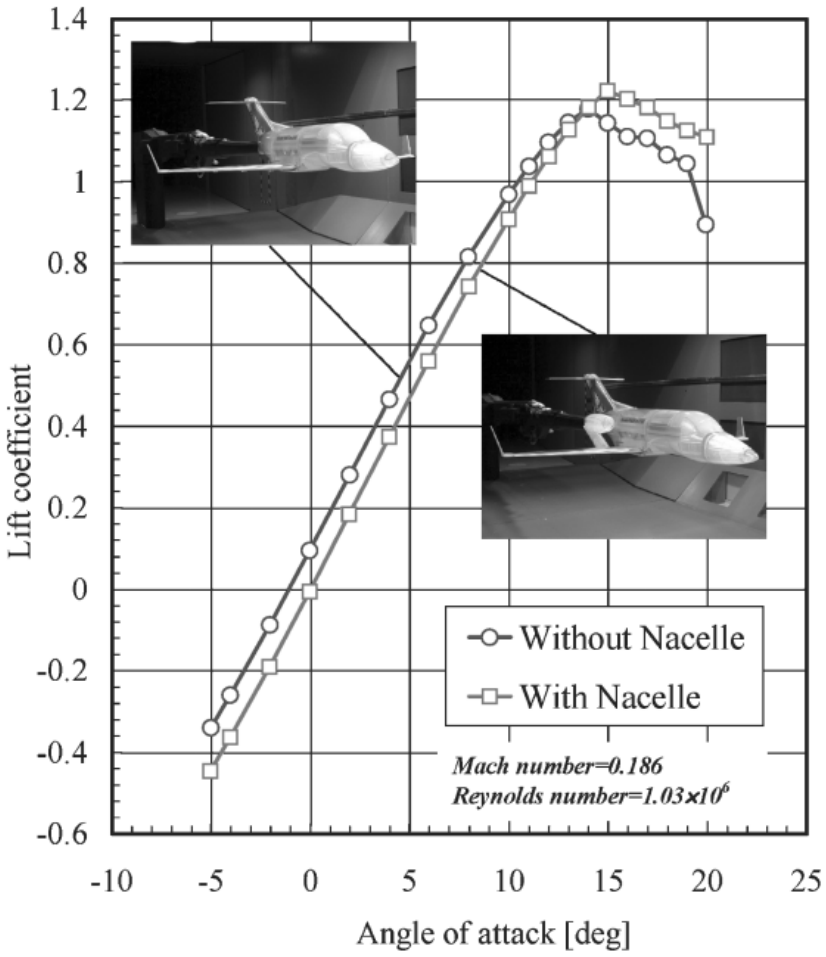

Figure 4.4: Experimental lift coefficient as a function of angle of attack[1]

As observed for the drag coefficient comparison, the numerical results for the lift coefficient do not match the experimental data. In particular, the simulated lift coefficients at angles of attack of 0° and 5° show significant deviations from the experimental measurements, indicating that the numerical model does not accurately capture the aerodynamic behaviour in this range.

4.1.3 Flow Distortion at the Engine Inlet

An analysis of the impact of the angle of attack on the airflow entering the engine was conducted[1]. Wind tunnel experiments have shown that the disturbance induced by the wing on the inlet flow only becomes significant at high angles of attack. This phenomenon is also observed in the numerical simulations.

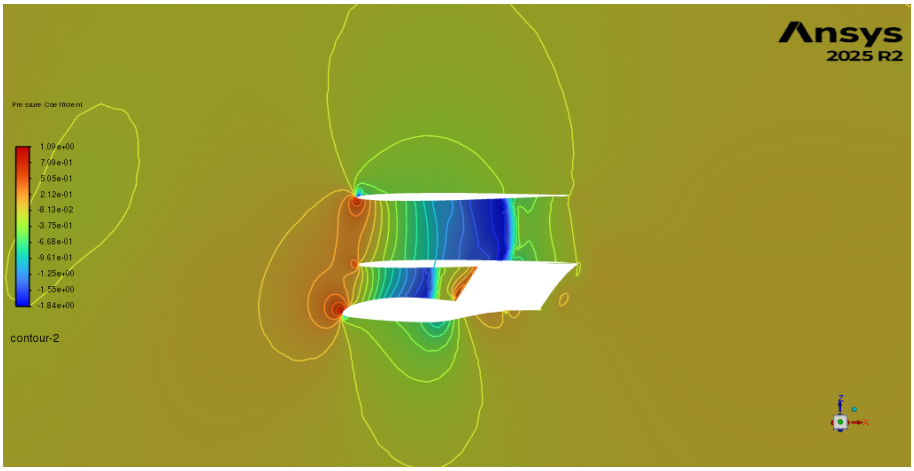

Figure 4.5: Pressure coefficient distribution near the engine inlet at high angle of attack

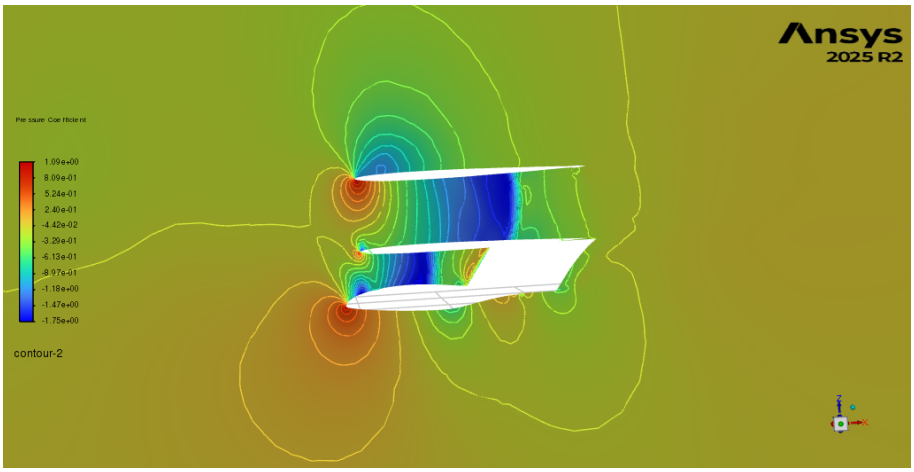

Figure 4.6: Detail of flow distortion at the engine inlet for $M = 0.7$

The turbulent flow generated by the wing induces a local pressure drop at the lower part of the engine inlet, leading to a distortion of the incoming flow. This effect becomes more pronounced as the angle of attack increases and may have implications for engine performance and stability.

4.1.4 Pressure Coefficient Distribution

The pressure coefficient (C_p) distribution is well captured by the numerical simulation. The computed results show good agreement with the wind tunnel measurements[1]. An example is presented for $M = 0.7$ and $Re = 10.2 \times 10^6$.

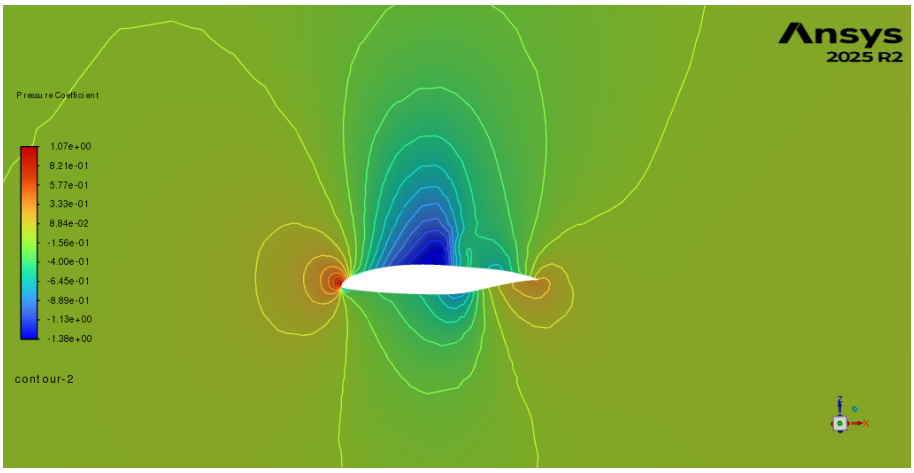

Figure 4.7: Numerical pressure coefficient distribution at $M = 0.7$

For all tested Mach numbers, the minimum and maximum values of C_p are similar. However, their locations and magnitudes vary with the angle of attack, reflecting the expected changes in aerodynamic loading.

4.1.5 Pressure Coefficient Distribution Along the Chord

In his study on Natural Laminar Flow (NLF) airfoils[3], Fujino presented pressure coefficient (C_p) distributions along the chord for various Reynolds numbers and Mach numbers.

Figures 4.10 and 4.9 show the C_p distributions obtained in the present study as a function of angle of attack and Mach number, respectively. Overall, the numerical simulations capture the pressure coefficient distribution reasonably well.

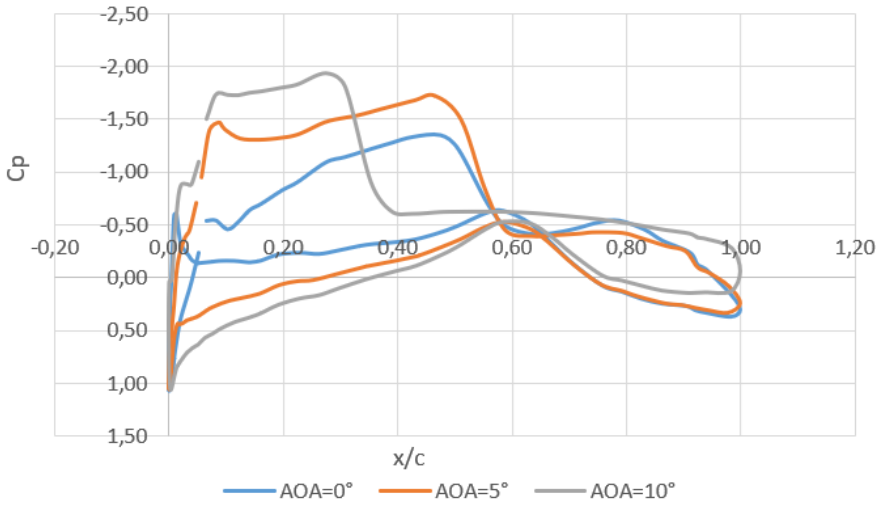

Figure 4.8: Numerical pressure coefficient distribution along the chord for different angles of attack

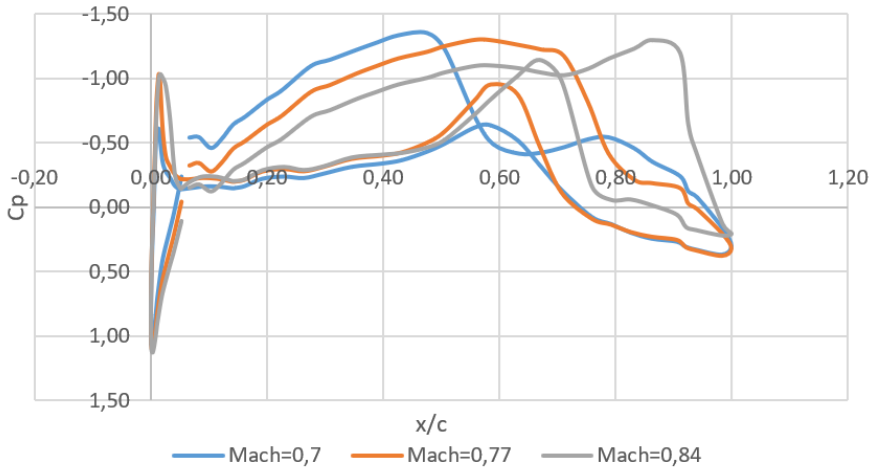

Figure 4.9: Numerical pressure coefficient distribution along the chord for different Mach numbers

4.2 Discussion and Limitations

The present numerical simulations do not perfectly reproduce the aerodynamic trends observed in the wind tunnel experiments. Several sources of discrepancy can be identified. First, the mesh resolution of the different aircraft components could be further refined to improve numerical accuracy. In addition, the turbulence model employed, namely the k–ω *SST* model, relies on inherent modelling assumptions that introduce additional uncertainties.

Despite capturing several qualitative aerodynamic features, the quantitative agreement with the experimental data remains limited. In particular, a systematic deviation by approximately a factor of two is observed in both the drag and lift coefficient results. This suggests that potential errors may exist in the implementation of the simulation parameters, such as reference areas, force normalisation, or boundary condition definitions.

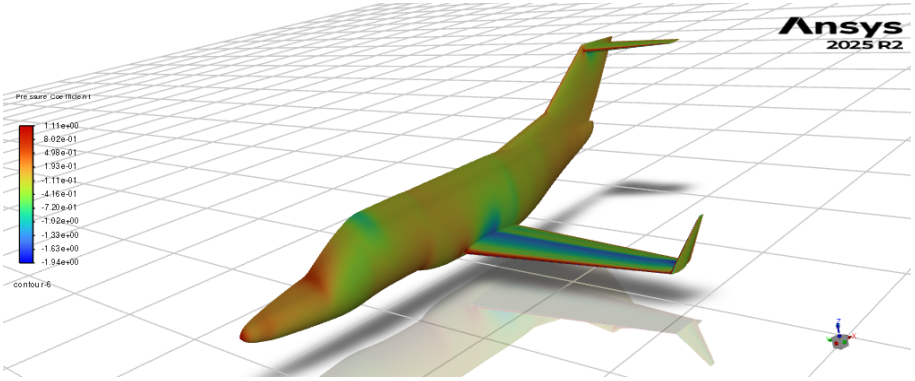

Figure 4.10: Numerical pressure coefficient distribution along the plane without engine at M=0.7

Chapter 5

Conclusion

This work investigated the aerodynamic behaviour of a regional aircraft configuration using Reynolds-Averaged Navier–Stokes simulations with the k–ω *SST* turbulence model under cruise conditions at 30 000 ft. A structured meshing strategy with body-of-influence regions was employed to ensure adequate resolution in key areas of the flow.

The numerical results were compared with wind tunnel experimental data. While the simulations successfully captured qualitative aerodynamic features such as pressure coefficient distributions and flow distortion at the engine inlet at high angles of attack, significant discrepancies were observed in the predicted lift and drag coefficients. In particular, the numerical values of C_l and C_d were approximately twice those measured experimentally.

These differences highlight the limitations of the current numerical setup, which may be related to mesh resolution, turbulence modelling assumptions, or the definition of reference quantities.

s

References

[1] Fujino M. Design and Development of the HondaJet. Journal of Aircraft. 2005;42(3).

[2] Teschner TR. Computational Arodynamics [Lecture]; 2025. Aerospace Computational Engineering. Available from: `https://cranfield.instructure.com/courses/37967`.

[3] Fujino M, Yoshizaki Y, Kawamura Y. Natural-Laminar-Flow Airfoil Development for a Lightweight Business Jet. Journal of Aircraft. 2003;40(4).

[4] Somers DM. Design of a Slotted, Natural-Laminar-Flow Airfoil for Business-Jet Applications. NASA; 2012. NASA/CR–2012-217559.

[5] Blaesser NJ, Schetz JA, Kapania RK. Interference Drag Associated with Engine Locations for Multidisciplinary Design Optimization. Hampton, VA: NASA Langley Research Center; 2020.

[6] Teschner TR. Computational Aerodynamics Assignment: Aerodynamic Performance of the HondaJet [Module Assignment];.